

Maunula, T., Ahola, J. and Hamada, H., Reaction mechanism and kinetics of NO_x reduction by methane on In/ZSM-5 under lean conditions, *Applied Catalysis B: Environmental*, 64 (2006) 13-24.

© 2006 Elsevier Science

Reprinted with permission from Elsevier.



Reaction mechanism and kinetics of NO_x reduction by methane on In/ZSM-5 under lean conditions

Teuvo Maunula^{a,*}, Juha Ahola^b, Hideaki Hamada^c

^a Ecocat Oy, Product Development, Typpitie 1, FIN-90650 Oulu, Finland

^b University of Oulu, Department of Process and Environmental Engineering, FIN-90014 Linnanmaa, Finland

^c National Institute of Advanced Industrial Science and Technology, Tsukuba Central 5, 1-1-1 Higashi, Tsukuba, Ibaraki 305-8565, Japan

Received 25 August 2005; received in revised form 21 October 2005; accepted 25 October 2005

Available online 28 November 2005

Abstract

Indium supported on ZSM-5 was investigated as a promising catalyst for NO_x reduction by methane under lean conditions. Indium on protonated H-ZSM-5 showed a higher activity in dry conditions while indium on unprotonated ZSM-5 with a high loading of 7.3% prepared by ion exchange had a higher activity in the presence of 8% water. NO₂ in feed promoted the methane oxidation and NO_x reduction. In situ FTIR analysis revealed on In/ZSM-5 the presence of inhibiting compounds at lower temperatures and many carbonaceous surface compounds. In the reaction initiation conditions, the surface coverage of nitrogen containing carbonaceous compounds and any adsorbed species were low. It is proposed that the formation of NO₂, partially oxidized methane surface derivatives and actual surface reductants containing N–C or N–H bondings are crucial in NO reduction. Intrazeolitic InO⁺ was proposed to be the active catalytic site in NO reduction. Free In₂O₃, detected by XRD and XPS, has possibly a promoting effect on the reactions. A micro kinetic model, including the surface intermediates, was derived for an In/ZSM-5 catalyst by the NO–CH₄–O₂ experiments where the reactant concentrations, space velocity and temperature were varied. The adsorbed H₂NCO intermediate, formed in the reaction between NO₂ and partially oxidized methane, was proposed to act as an actual NO reductant in the reaction mechanism and kinetic equations. The model was able to follow measured responses and predict the dynamic performance in NO–CH₄–O₂ reactions quantitatively in usual steady state lean conditions. Adsorbed oxygen and NO₂ were simulated to exist with higher coverage on active sites in reaction conditions. Gas and adsorbed compounds were simulated as a function of reactor length in different unmeasured conditions, which simulations can be used as a tool in catalyst reactor design.

© 2005 Elsevier B.V. All rights reserved.

Keywords: Nitrogen oxides; Selective catalytic reduction; Methane; Indium; ZSM-5

1. Introduction

The emission standards for harmful nitrogen oxides formed by combustion of fossil fuels in engines and power plants are becoming stricter these days. Although small-sized natural gas power plants or engines have low fuel consumption with less additional costs in lean combustion conditions, the treatment of emitted NO_x is a difficult problem to solve. This is because the three-way catalyst does not work in lean conditions and SCR with ammonia is not practical for small-scale combustors due to ammonia being poisonous.

In this regard, NO_x reduction by different types of hydrocarbons on zeolite and oxide based catalysts has given promising results even in the presence of excess oxygen [1,2]. For NO_x reduction in real exhaust gases, unsaturated hydrocarbons are usually more reactive than saturated hydrocarbons such as methane and ethane used as reductants [3]. Therefore, durable and selective catalysts for NO_x reduction by methane (CH₄-SCR) in lean conditions can be a key improvement in order to achieve environmentally friendly low-emission power plants and natural gas fuelled vehicles.

Pd/H-ZSM-5 has been reported to be an active catalyst for NO reduction by CH₄ in the presence of oxygen [4–6]. Li and Armor [7–9] showed that cobalt and gallium ion exchanged ZSM-5 and ferrierite catalysts are active for the

* Corresponding author. Tel.: +358 10 6535786; fax: +358 10 6535700.
E-mail address: teuvo.maunula@ecocat.com (T. Maunula).

same reaction. Kikuchi et al. [10–12] proposed bi-functional reaction mechanism for NO reduction by methane over indium and gallium on H-ZSM-5. In their study, NO has been proposed to be oxidized to NO₂ on zeolite and the NO₂ is reduced to nitrogen on Ga or In sites. Thus, the oxidation of NO to NO₂ is now generally accepted to be an important reaction step to improve NO_x reduction by methane [13–15]. It is proposed that indium is distributed inside ZSM-5 channels, interacting with zeolitic Brønsted acid sites and producing Lewis sites, which amount correlates to the highest activity [16]. Two kinds of indium sites in In/HZSM-5/In₂O₃ showed remarkable activity for CH₄-SCR of NO_x [17]. Indium has a role to enhance the adsorption of NO_x species at reaction conditions. Intrazeolite indium oxo species (InO⁺) are active CH₄-SCR sites [18]. Multifunctional catalysts have also been introduced for the same reaction, e.g. by the addition of Co on Pd/H-ZSM-5 [19], Pt on In/H-ZSM-5, Ir on In/H-ZSM-5 or CeO₂ on In/ZSM-5. In/H-ZSM-5 itself is already a bi-functional catalyst having proton and In sites. A kinetic model for In/ZSM-5 has been introduced earlier in a publication by using power law equations with CH₄, NO, O₂ and possibly with H₂O concentrations [20].

In addition, promising NO_x conversions in the presence of methane have been found with Rh, Mn, Ni, Ce and Ag ion exchanged ZSM-5 in lean conditions [21–23]. Concerning non-zeolite catalysts, many experiments have been made with metal oxide based catalysts like Pd/TiO₂, La/Al₂O₃, Sr/La₂O₃ and rare earth oxides for the same reaction [24–27]. NO_x reduction by different hydrocarbons on multi component catalysts has been proposed in several publications, where an efficient HC-SCR catalyst has been combined with good oxidation catalysts [28–33].

In/ZSM-5 catalysts showed in our preliminary experiments a particularly high activity for NO_x reduction and therefore more detailed investigations have been under taken to understand the key points in catalyst composition and reaction mechanism. The kinetics of NO_x reduction by methane on In/ZSM-5 has been examined by laboratory experiments and a micro kinetic model was derived based on the detected and assumed gas phase compounds and surface intermediates.

2. Experimental

2.1. Catalyst preparation

Protonated (H form) and unprotonated (Na form) ZSM-5 (Tosoh, SiO₂/Al₂O₃ = 23) was used as a zeolite support for catalysts. Washed ZSM-5 or H-ZSM-5 zeolite was ion exchanged in 0.04 M In(NO₃)₃ solutions at 80–90 °C for 24 h, dried and calcined at 500 °C for 3 h. The ion exchange ratio (IER) of In³⁺ was calculated to be about 140% on In/ZSM-5 and 55% on In/H-ZSM-5 by quantitative RF (Seiko Instruments SEA2010) and plasma analysis. Possibly the higher preparation temperature had enhanced the ion exchange of indium.

2.2. Characterization

The surface area (BET) was determined by the nitrogen adsorption at –196 °C (Micromeritics Flow Sorb II) after pretreatment in N₂/He flow at 300 °C for 30 min. Metal and oxide phases were detected by XRD analysis (Shimadzu XD-D1), where powder samples were analyzed using a Cu Kα target and a 0.6 mm received slit by the rotation speed of 2° min⁻¹. The state of indium species on surfaces was evaluated by the binding energies of In3d_{5/2} in XPS analysis (Rikagaku Denkiogyo XPS-7000). In addition, the combined values of the binding and kinetic energies were used for the evaluation, where pure metallic In and In₂O₃ were used as references. The baseline and the pretreatment pressure was 3 × 10⁻³ Pa at 25 °C.

2.3. Activity experiments

The steady-state activity of the powder catalysts was measured in a quartz flow reactor using simulated exhaust gases containing about 1000 ppm NO or NO₂, 1000 ppm methane and 10% oxygen in helium in the temperature range of 200–600 °C. In some experiments, 500 ppm N₂O replaced NO_x and oxygen was absent (NO and N₂O decomposition studies) in the gas mixture. The exact feed composition (NO, CH₄ and O₂ inlet) was analyzed by GC in each experiment and the calibrated value was used in conversion calculations and kinetic experiments instead of the nominal concentration values. The fluctuation was about ±10% compared to the nominal values. Temperature was measured directly by a thermocouple located in the sample bed. Total gas flow rate (*F*) was 66 ml/min and the amount of a sample (*W*) was 0.2 g resulting in *F/W* to be 20 dm³ h⁻¹ g⁻¹ in a standard mixture. The particle size was screened to a fraction <250 μm to prevent mass transfer limitations in the particles, even if the studied molecules were very small. In kinetic experiments, the concentrations and *F/W* (changed by *W*) were varied in the following ranges: 500–1000 ppm NO, 500–2500 ppm CH₄, 4–10% O₂ and 20–240 dm³ h⁻¹ g⁻¹ *F/W*. The composition of outlet gas (N₂, N₂O, NO, NO₂, CO₂, CO and CH₄) was analyzed using two gas chromatographs (Shimadzu GC 8A with Porapak Q and Molecular sieve 5A columns) and a chemiluminescence NO_x/NO analyzer (Shimadzu NOA-305A) [34]. The formation of nitrogen (N₂) and CO_x (CO and CO₂) was analyzed to interpret the selectivity in CH₄-SCR. It is assumed that the hydrocarbons reacted up to gaseous CO_x, have been lost as reductants in lean conditions.

2.4. FTIR studies

The reactants (NO, methane and oxygen) were introduced inside of an in situ FTIR chamber in sequential steps at constant temperatures between 50 and 450 °C and the adsorption bands of formed surface species in those static conditions were measured on evacuated samples. FTIR spectra were measured in the wave number range of 4000–1000 cm⁻¹ by Shimadzu FTIR-8600PC equipped with a liquid nitrogen cooled detector

using a resolution of 4 cm^{-1} . The powder samples (0.1 g) were pressed to thin, infrared-light transparent discs, which were installed at right angle to beam in the middle of a quartz reactor equipped with NaCl windows and a thermocouple in a pocket located inside the chamber. Before adsorption the sample was out gassed at $480\text{ }^{\circ}\text{C}$ for 30 min to remove moisture and contamination, then it was cooled to the set-point temperature (50, 150, 250, 350 and $450\text{ }^{\circ}\text{C}$), where a background spectrum was first measured in vacuum ($<2 \times 10^{-3}$ Torr). Pure NO (>99%), methane (>99%) and oxygen (>99.9%) were introduced separately at the partial pressure of 20 Torr into the chamber by the sequence: $\text{NO} \rightarrow \text{CH}_4 \rightarrow \text{O}_2$. Each gas was allowed to adsorb and react for 10 min and then the chamber was evacuated for 5–10 min before a new gas dose. The first gas in sequence was adsorbed on the pretreated, pure surface but the next gases were introduced on the surface with adsorbed species. FTIR spectra were measured during each step after 2 and 10 min. Adsorption bands of the single gases (NO, CH_4 , CO, N_2O , N_2 and CO_2) on pretreated In/ZSM-5 and ZSM-5 were also recorded at $50\text{--}350\text{ }^{\circ}\text{C}$ as our own reference to explain observed peaks in reaction studies.

The dynamic in situ FTIR reaction studies were performed in the same chamber, which was equipped with a feed of flowing gases. The pretreatment (evacuation at $480\text{ }^{\circ}\text{C}$ for 30 min) and FTIR parameters were the same as in the static experiments. The background spectrum was measured at $200\text{ }^{\circ}\text{C}$ in an He flow. The diluted reaction gases were introduced in a sequence of O_2 , NO and CH_4 in the chamber and the final composition and flow rate were about the same as in

the activity test reactor, approximately 1000 ppm NO, 1000 ppm CH_4 and 9.3% O_2 in He (total flow rate 62–66 ml/min). The reaction gas was mixed by mass flow controllers using 3050 ppm NO/He, 3.06% CH_4 /He and 30.8% O_2 /He as source gases. FTIR spectra were measured in the flowing gas mixture at about 200, 240, 280, 320, 360, 400, 440 and $450\text{ }^{\circ}\text{C}$, while the temperature was elevated at the rate of $10\text{ }^{\circ}\text{C}/\text{min}$. The measurement of every single spectrum took about 2 min corresponding to the average IR data of the temperature range of $20\text{ }^{\circ}\text{C}$. The mass spectrometer (MS) was connected to the system, but it was difficult to detect other than main gas compounds (CH_4 , NO and CO_2) because of the overlapping of the masses and low concentrations of the side products. The main gaseous compounds were also observed qualitatively by FTIR.

3. Results and discussion

3.1. Reaction experiments

3.1.1. NO reduction by CH_4 in dry and wet conditions

In/H-ZSM-5 had a higher activity in dry conditions than In/ZSM-5 even though it had a lower ion exchange ratio of indium. This can be explained by its higher amount of free zeolitic acid sites [12], which can enhance NO oxidation to NO_2 and CH_4 adsorption in dry conditions (Fig. 1). In/ZSM-5 contained still sodium and the amount of protonated sites was lower after preparation, because it was not pretreated in ammonium nitrate solution and the indium concentration was

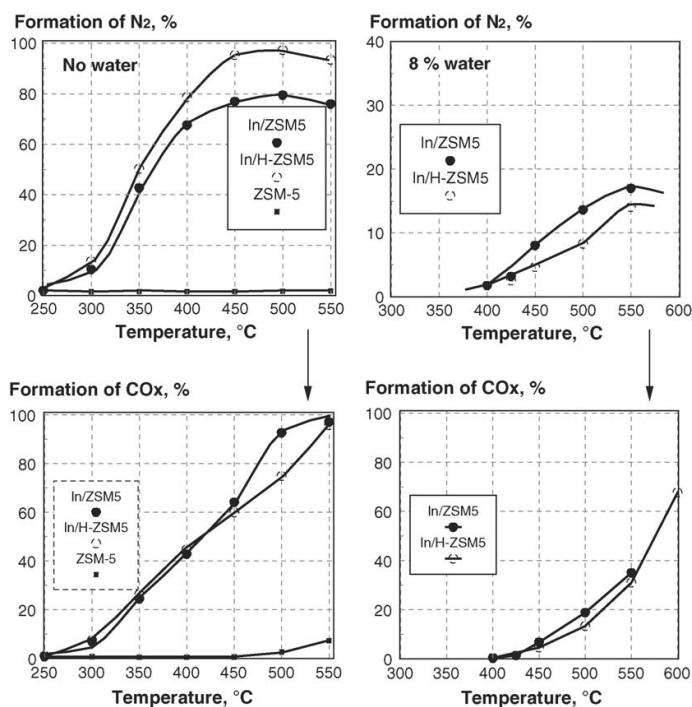


Fig. 1. The N_2 and CO_x formation in $\text{NO-CH}_4\text{-O}_2$ reaction on ZSM-5 supported In catalysts in dry and wet conditions.

higher than with In/H-ZSM-5. Since the ion exchange ratio in In/ZSM-5 was 140%, indium was assumed to locate partly on Si sites in zeolite framework or the ion exchange did not follow exactly the assumed ratio (an In^{3+} ion per three Na^+ ions). This observed difference showed that it is easier to ion exchange indium with higher concentrations into ZSM-5 (untreated) than into H-ZSM-5 (protonated) zeolite in normal preparation conditions. Na and H were mainly replaced by indium in preparation but the supports were denoted in this paper according to the initial zeolite state. The protonated zeolite state (H-ZSM-5) in the indium addition step is assumed to favor the formation of intrazeolite InO^+ [13], creating the high catalytic activity. The conditions of the ion exchange process in our study favored the intra zeolitic indium formation similarly as observed by Schmidt et al. [35].

The light-off temperature (T_{50}) of methane on In catalysts was around 400 °C in dry and 580 °C in wet exhaust gases. Therefore, water prevents the methane oxidation in the range of 400–550 °C. When 10% water was added in the gas mixture, the NO_x conversion to nitrogen was decreased to less than 20% and the NO_x reduction window was shifted about 100–150 °C to the higher temperatures on these In/zeolite catalysts. It is noted that the activity of In/ZSM-5 (7.2% In) was higher than that of In/H-ZSM-5 (2.7% In) in the presence of water. The higher In loading in In/ZSM-5 was a reason for the higher stability in wet experiments. Generally it can be assumed that higher In loadings are needed to catalyze these reactions in wet conditions. Proton sites, present on the fresh catalysts, are assumed to be unstable in real exhaust gas conditions in the presence of water, sulfur and other deactivating compounds. It was reported that sodium can increase the NO adsorption compared to propene adsorption on zeolites, which property can be beneficial in the studied application [36]. The higher activity drop of Pd/H-ZSM-5 compared to Pd/Na-ZSM-5 caused by aging was reported earlier for the same reaction [37], which is an example about the stability of Na-ZSM-5 also used as a support in this study. Even if the long-term activities in the presence of real exhaust gases were not examined in this study, the short-term experiments in the presence of water confirmed us to use In/ZSM-5 in the following reaction studies. However,

these results in wet conditions showed the general problem of CH_4 -SCR in practical applications.

3.1.2. NO_2 and N_2O reduction by CH_4

Indium-free ZSM-5 had no activity either for NO or NO_2 reduction by methane in the presence or absence of oxygen. This was also a clue that only few or no protonated zeolite sites exist on untreated ZSM-5. The activity of In/ZSM-5 was improved to the same level with In/H-ZSM-5 when NO was changed to NO_2 in feed (Figs. 1 and 2). This comparison showed likewise that the NO oxidation was a limiting reaction step on In/ZSM-5 in $\text{NO}-\text{CH}_4-\text{O}_2$ mixture. The N_2O experiments showed that nitrous oxide was preferably reduced by methane ($T_{50} = 470$ °C) or directly decomposed to N_2 ($T_{50} = 550$ °C, when no CH_4 present) on In/ZSM-5. According to these experiments, N_2O route did not explain the observed high activities of In/ZSM-5 for NO_x reduction in lean conditions. However, N_2O formed as a side product from NO_x in lean mixtures will be reduced to nitrogen above 450–500 °C. Indeed, a low amount of N_2O (20 ppm at 350 °C) was detected with our standard $\text{NO}-\text{CH}_4-\text{O}_2$ mixture at lower temperatures, when the NO reduction by methane is initiating.

3.1.3. The role of oxygen and side products

The temperature had to be over 600 °C on this catalyst to reduce NO by methane to N_2 in the absence of oxygen (Fig. 2). Therefore In/ZSM-5 is a very poor catalyst to remove NO_x under stoichiometric or rich conditions, where noble metal catalysts are more active. A reason for the observed low activity in rich conditions can be strongly adsorbed NCO or other rich side species, which will be decomposed in the presence of water and precious metals. Thus, the efficient NO_x reduction on this catalyst requires the presence of oxygen. Oxygen is needed to oxidize carbonaceous species on catalyst surface and to oxidize NO to NO_2 , which is a very reactive oxidizer for methane and its surface derivatives. The maximum CO concentration was 0.3% with NO and 0.8% with NO_2 in feed. Small quantities of CO were formed from methane but it is not an important gas phase intermediate for NO_x reduction because it is unselective in lean SCR reactions [45].

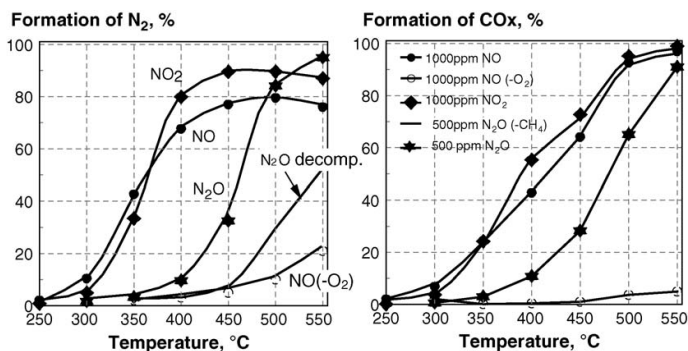


Fig. 2. The reduction and decomposition of NO, NO_2 and N_2O to nitrogen by methane on In/ZSM-5 in dry conditions (if present, 10% O_2 and 1000 ppm CH_4 ; $-\text{CH}_4$; no CH_4 , $-\text{O}_2$: no oxygen in feed).

Table 1
Composition of the catalysts used for NO reduction by methane

Catalyst	In loading (wt.%)	BET (m ² /g)
In/ZSM-5	7.2	269
In/H-ZSM-5	2.7	303
ZSM-5	–	219

3.2. Characterization of In/ZSM-5

The surface area (BET) of In/H-ZSM-5 was higher than that of In/ZSM-5, for which the high indium concentration probably decreased the surface area (Table 1). Indium on protonated ZSM-5 had surface area over 300 m²/g, which can be attributed to sodium removal both in the treatment with NH₄NO₃ and the indium ion exchanges process as well as to a lower indium concentration. Larger In₂O₃ particles have a low surface area and they will decrease the total surface area. Plasma analysis showed that In/ZSM-5 contained still 0.63 wt.% sodium. The amount of sodium in untreated ZSM-5 was 2.3 wt.%. Therefore, only 73% of sodium was removed during the indium ion exchange process to prepare In/ZSM-5 even if the calculated IER was 140% in that sample. We assume that the removal of sodium was a reason why In/ZSM-5 and In/H-ZSM-5 had a higher surface area than ZSM-5 but this observation can be also related to the effects of BET pretreatment on these samples, because zeolites are very sensitive to moisture removal and sodium can have an effect.

In₂O₃ was detected as a main compound on In/ZSM-5 by XRD (Fig. 3). Silica rich ZSM-5 structure was also confirmed according to the peaks in the literature data [8]. No indium metal peak was found on the analyzed In/zeolite samples. However, finely dispersed, intrazeolitic species can be undetectable by XRD, which thus observed only the large In₂O₃ particles on ZSM-5. According to the binding, kinetic and calculated combined energies in XPS analysis, indium was clearly nearer to In₂O₃ than metallic In on ZSM-5 (Table 2). A slight shift in the spectra between reference In₂O₃ and the

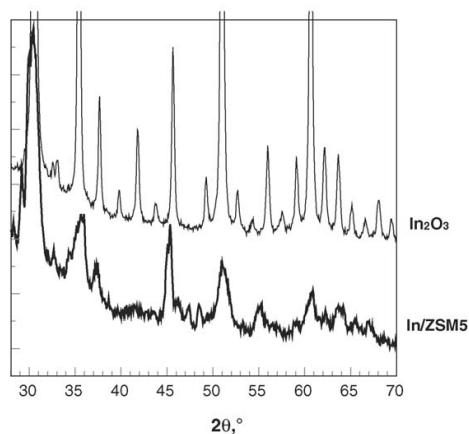


Fig. 3. XRD characterization of In/ZSM-5.

Table 2

The XPS binding, kinetic and calculated combined energies for fresh indium samples (eV)

Sample	In3d _{5/2}	InA(MNN)	In3d + InA K.E.	O1s	Al2p	Si2p
In/ZSM-5(500)	444.8	848.6	850.8	532.8	75.0	103.7
References						
In ₂ O ₃	444.3	846.7	851.2	529.9		
In metal	443.6	842.8	854.4			

Cl1s = 285.0 eV chemical shift reference.

sample can be caused by the interaction between zeolite and indium oxide structures. According to these XRD and XPS characterizations, In₂O₃ was the main detected phase in In/ZSM-5. However, InO⁺ has been detected to be the active site in the investigated reaction in earlier studies [38,39], which can be related to the energy value shift by XPS analysis. Because In/ZSM-5 samples in our study contained high concentration of In (IER > 100%), it is probable that InO⁺ exists near to zeolitic Al sites and at the same time, In₂O₃ on the external surface of ZSM-5. In addition, InO⁺ is evidently a more important active site in In/H-ZSM-5 with IER of 55%. Even if In₂O₃ was detected as the main stable phase at room temperature, the active sites like InO⁺ are obvious, particularly in dry reaction conditions at high temperatures (400–600 °C).

According to our characterizations, there exist at least the following sites, which have catalytic properties: H, Na and In in ZSM-5 and In₂O₃ particles on ZSM-5. It can be assumed simply by the calculated IER in In/ZSM-5 that In is not solely in zeolite pores but also as separate particles in extra zeolitic locations. The particle size and stability of these extra zeolitic In₂O₃ sites are not known but the observed activity was higher in wet conditions with In/ZSM-5 having high IER. It is assumed that there exist two types of In sites, which have seen to promote NO reduction also by Ren et al. [17]. The observed high activities in our study were evidence about the multifunctional catalysis. However, these multifunctional properties were lumped in the kinetic equations for simplicity and the model will still be able to explain the reaction dynamics.

3.3. Reaction intermediates

3.3.1. Static NO–CH₄–O₂ measurements

Single molecules (NO, CH₄, O₂, CO, CO₂ and N₂O) as gas and adsorbed species on ZSM-5 and In/ZSM-5 were detected at 50–350 °C to make an internal spectrum library for our FTIR equipment. This own spectrum database was a tool to trace the reaction intermediates in the static and dynamic measurements in used experimental conditions in addition to published FTIR spectrum literature, where the data are measured mainly at room temperature. The number and intensity of peaks of adsorbed species decreased with these single gases when temperature was increased from 50 to 350 °C.

The possible surface species according to single gas and literature spectra are (ads = adsorbed):

In-CO₂ or CO₂ gas: 2345–2355 cm⁻¹
 In-CN, Si-NCO: 2303 cm⁻¹ [11]
 In-NO, -CN: 2137 cm⁻¹
 ads (ONO) on InO⁺: 1622 cm⁻¹ [16]
 ads NO₂ on InO⁺: 1575 cm⁻¹ [16]
 Ads N₂O₄ on Na/M-ZSM-5: 1740 cm⁻¹ [16,40]
 ads-CO_x: 1980 cm⁻¹
 ads-NO_x: 1865–1870 cm⁻¹
 ads CHO: 1695–1700 cm⁻¹
 ads HNCO: 1640–1650 cm⁻¹
 NO₃⁻-H⁺: 1680 cm⁻¹ [16]
 structural O, H, C, N: 1700–1600 cm⁻¹
 structural O, H, C: 1520 cm⁻¹

A comparison of static measurements after dosing NO, CH₄ and O₂ in sequence and evacuation on In/ZSM-5 is shown in Fig. 4. The peaks in the range of 4000–3500 cm⁻¹ showed the acidic sites on ZSM-5. The existence of aluminum in tetrahedral coordinated silicon structure requires a charge compensating cation which is originally sodium and can be ion exchanged to various other metal cations accessible to zeolite framework [9]. Hydroxyl groups in zeolite have been recognized as a main source of acidity. Zeolite lattice oxygen ions and occluded alkali metals form zeolite basic sites, which have also been reported to have an ability to catalyze hydrocarbon reactions. ZSM-5 and other zeolites used for NO reduction by hydrocarbons are hydrophobic which means that they can selectively adsorb hydrocarbons even in the presence of water steam. The dosing of CH₄ on an NO treated sample created clearly a higher peak around 3740–3744 cm⁻¹. The observation that the spectra on In/ZSM-5 were very similar to the ones on alumina based catalysts [31] proofed that aluminum dominates to silicon as an adsorption site on ZSM-5. The fact that the reactants are adsorbed in certain sequences (NO ads → evacuation → CH₄ ads → evacuation → O₂ ads → evacuation) can limit the reactions compared to a flowing mixture of these compounds. The lack of gaseous oxygen during NO and methane adsorption steps can have

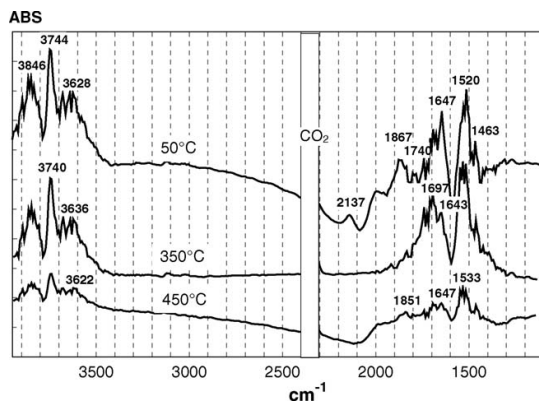


Fig. 4. Static FTIR measurements in vacuum on In/ZSM-5 at 50, 350 and 450 °C after dosing 20 Torr NO, 20 Torr CH₄ and 20 Torr O₂ evacuation after each dose.

limited the formation of oxygen rich species. The intensity of the detected compounds was decreased when temperature was risen showing the weaker bonding and desorption of adsorbed species. Adsorbed water formed by reactions or as an impurity can have caused a part of the observed peaks in the same range, particularly at lower temperatures.

In-NO or In-CN (2137 cm⁻¹), adsorbed NO_x on In (1867 cm⁻¹) was detected at 50 °C but no longer at higher temperatures. Structural or adsorbed C–H–O (e.g. 1520–1533, 1697 cm⁻¹) and C–H–O–N (e.g. 1645 cm⁻¹) species are stable up to 350–450 °C. Adsorbed N₂O₄ on zeolitic Na sites was possibly present at 1740 cm⁻¹. Carbonate caused the peaks at least around 1480 cm⁻¹ according to our single gas library. It is assumed that adsorbed C–N, N–C–O, (N_xO_y)_z or organic nitro/nitrile intermediates react directly or with NO to form N₂. However, when the reaction rates were the highest, the detection of any adsorbed species was limited. Often when a strong adsorption band of certain reactants is observed, the NO reduction is limited by inhibition, because strongly adsorbed species prevent the initiation of chain reactions. As many detected carbonaceous species are the side products relating to proposed reaction paths, they will not be defined in our reactions used for modeling.

3.3.2. Dynamic NO–CH₄–O₂ measurements

In/ZSM-5 was analyzed in situ in the presence of flowing NO–CH₄–O₂–He, CH₄–O₂–He and He gas mixtures in a temperature ramp from 200 to 480 °C. The activity experiments and FTIR studies can be linked directly together because the inlet concentrations were the same in both experiments. The three experiments were used in the spectra comparisons, where the spectrum in He flow was subtracted from NO–CH₄–O₂–He or CH₄–O₂–He spectrum (Figs. 5 and 6). Therefore, the effect of NO in the gas mixture might be found by this comparison. The effect of temperature in the experiments was eliminated with this He-only experiment, where it was also detected peaks caused by distortions or collision assisted desorption (negative peaks) during a temperature ramp (background at 200 °C). The presence of NO in the feed caused a kind of negative distortion on FTIR spectrum at lower temperatures. Thus the

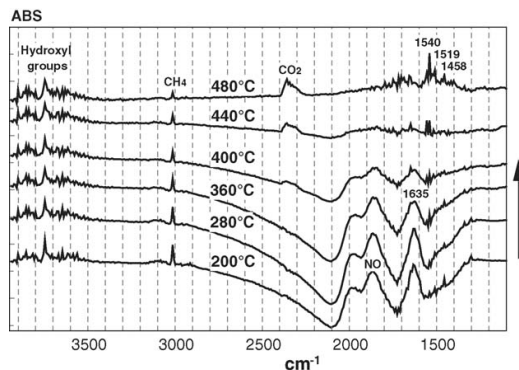


Fig. 5. Difference spectra of NO–CH₄–O₂–He minus He at 200–480 °C in flowing gas on In/ZSM-5.

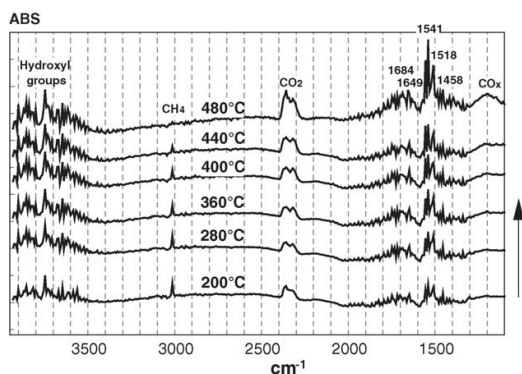


Fig. 6. Difference spectra of $\text{CH}_4\text{-O}_2\text{-He}$ minus He at 200–480 °C in flowing gas on In/ZSM-5.

higher temperatures (400–480 °C) are clearer to be compared in the presence and absence of NO. The spectrum showed the gas phase changes during temperature rise: the reduction of NO gas (about 1800–1900 cm^{-1}) and the formation of CO_2 (2360 cm^{-1}) from methane (3014 cm^{-1}). The presence of gas phase compounds can have overlapped a part of adsorbed species in the spectrum. These experiments confirmed that carbonaceous (C–H–O) compounds are the main adsorbed species and the nitrogen containing compounds are not the main adsorbents on the catalyst surface in the reaction conditions. Of course, it was limited possibilities to detect which compounds were located on the In sites because zeolite support is the main phase which could act as a “pump” of C–H–O compound to the In sites. It is assumed that a higher coverage of these carbonaceous compounds are needed to form reducing conditions on catalyst surface to cut the N–O bonding and to create N–C and N–H bonded adsorbed species, which are able to reduce NO. Further more, it can be proposed by these FTIR observations that the coverage of these nitrogen containing species will never be very high because they will react fast with NO to N_2 , desorb or be re-oxidized back to NO_x species depending on the conditions. Partially oxidized hydrocarbons were formed at lower temperatures but they disappeared around 400–450 °C and they might contain a low amount of nitrogen. The adsorption of carbonates on In/ZSM-5 was higher in the absence of NO. It is reported that ZSM-5 is able to adsorb nitrate species (1680 cm^{-1}) at lower temperatures but these compounds will disappear before the reaction operation temperatures [16]. Therefore, adsorbed nitrates are not the key compounds in the reactions but the opposite they are the compounds, which inhibit the initiation of the desired reactions. In the same study it was detected that NO_2 and NO_3^- adspecies on InO^+ are still present around at the reaction temperature. Nitrates are an NO_2 reserve on the catalyst surface. In our experiments these species were possibly present up to 400 °C but not at higher temperatures. The comparison between these spectra showed that the peaks of 1800–2000 and 1630 cm^{-1} were created by the influence of NO. In situ FTIR showed the existence of mainly C–H–O, adsorbed NO_x , and N–

C–H–O species, when the NO conversion rate was highest in the activity experiments at 400–480 °C.

3.4. Reaction mechanism

The reaction pathways have been proposed based on reaction mechanism including surface reactions and all the intermediates are exactly defined by reaction stoichiometrics (no undefined “X” compounds). Kinetic modeling was used as a tool to verify the proposed surface reactions based on experimental detections and to analyze the reaction dynamics quantitatively both in observed and unmeasured conditions. If the proposed reaction mechanism correctly includes the main features of the actual reaction pathway, the model should be able to show the reactant and product responses in defined conditions. The methane oxidation is simpler to model than the propene oxidation and the number of possible parallel reaction routes is much lower with methane. Thus, it was possible to take into account the main steps into methane oxidation and carbon–nitrogen fixation. Hydrogen and carbon in CH_4 react to water and CO_x in several reaction steps parallel to the final nitrogen formation. The methane oxidation has been described by the single reactions where water and CO_2 are formed as final products. OH^* type surface intermediates are excluded because of simplicity. However, it is difficult to activate C–H bond in methane, because the C–H bond strength is higher in CH_4 than in other hydrocarbons and it has a low ability to be adsorbed on surfaces [41]. The hydrocarbon cracking is connected to Brønsted acid sites of ZSM-5 [42].

Oxygenated methane derivatives were detected by FTIR studies at temperature, where methane oxidation and NO_x reduction initiated. Qualitative experiments showed that NO_2 has a remarkable role in HC oxidation therefore, NO_2 as an oxidizer has been emphasized in the reaction paths. N_2O was excluded as a key intermediate to dinitrogen.

In/ZSM-5 has at least two types of active centers (zeolitic acid and In sites) but because the contact of these sites is needed and In/ZSM-5 is much more active than ZSM-5, we are proposing that the catalyst is containing only one active site: Indium on ZSM-5 (denoted as *). However, the support interaction with indium oxide is a key to the high activity and stability.

In reality, many reaction pathways exist at the same time but the proposed reaction mechanism was common enough to interpret the kinetic limitations and the stoichiometry in reaction sequences can be kept in balance. Based on these assumptions, the reaction mechanism can be proposed as shown below.

Adsorption both on metallic and oxidized indium site has been considered. Methane is proposed to be adsorbed only on an oxidized site. The adsorption of methane and nitrogen components on acidic sites of the zeolite is not an explicit part of the proposed mechanism. Adsorption steps are as follows:



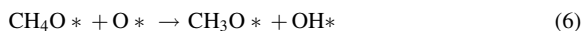


Nitrogen dioxide can be formed reversibly from nitric oxide

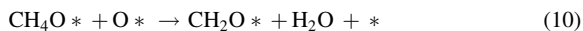


in which the equilibrium constant was defined in such a way that, together with adsorption steps, the thermodynamic equilibrium gas phase composition will be asymptotically achieved.

The oxidation of adsorbed methane is proposed to be started with oxidative dehydrogenation, in which two hydrogen atoms are removed from methane [43]. The oxidative agent can be adsorbed oxygen, nitrogen dioxide and hydroxyl radical.



The reaction of hydroxyl with adsorbed CH_4O as well as the reaction of adsorbed oxygen or nitrogen dioxide with CH_3O is also possible. NO_2 has been proposed to enhance H-abstraction from methane similarly also in gas phase [44]. However, the reactions of hydroxyl with CH_3O^* and dissociation of HNO_2^* were proposed to be fast. Thus, we were able to aggregate the several steps to two reaction steps:



These steps explain the increasing methane oxidation rate, when NO_2 is present in reactive mixture. The complex CH_2O^* is proposed to be a component, which is able to create the actual NO reductant.



The nitrogen containing hydrocarbon complex NCH_2O^* is proposed to react further with NO^* by competitive reactions:



in which gaseous nitrogen or nitrous oxide is formed. The reaction steps (12)–(14) form a catalytic cycle, in which the hydrocarbon species do not actually reduce the nitric oxide but behave as catalytic agent in the NO decomposition. The cycle increases the amount of oxidized sites, which shall be recovered to reduced sites. The reducing agent is proposed to be CH_2O^*



The rate of this reaction step is crucial on the reduction efficiency of a catalyst. If the rate is too high compared to the rate of NO decomposition cycle, the NO reduction selectivity is poor and that kind of catalyst behaves as a methane oxidation catalyst. On the other hand, if the rate above is too slow the reduction selectivity is good but total activity of catalyst become poor, because the catalyst surface will be covered with oxygen. The CH_2O^* intermediate is a junction, where methane derivatives will proceed to form CO^* or NCH_2O^* in the reaction sequences.

The overall catalytic cycle shall be completed with carbon monoxide oxidation and desorption



The scheme of NO reduction with methane on In/ZSM-5 proposed by Kikuchi et al. [12–15] matches our more detailed reaction mechanism especially for methane reactions where many other pathways can explain the observed reactions. Particularly the N containing surface intermediates which can have different bond configurations but have the same chemical compositions. The main assumption is that the N–O bonding from the N origin (NO) is broken and N is bonded to C or H. In lean conditions NH_i type compounds (amines) are known to be selective for NO reduction, meaning that the actual reductant has the configuration of H_2NCO . This kind of reaction scheme can be proposed in general for HC-SCR because the final actual reductant is the same that we proposed for NO reduction with propene on Co/alumina [45]. Therefore, the efficient NO reduction requires selective reductants on the catalyst surface similarly as in NH_3 -SCR, where adsorbed NH_2 is also the actual reductant for NO. The catalysts are completely different than in NH_3 -SCR, because we need the zeolitic properties to create in situ the actual reductants in HC-SCR. We assume that nitro and nitrate species observed in publications might preclude these actual reductants but they are not able to reduce NO. Nitromethane has been explained to react through HNCO to NH_3 on alumina [46] and M/ZSM-5 [47] which observation also supports our assumption. The electronic states can be also balanced by surface site *, which can be, e.g. as an oxide form. NO_2 could also move through the gas phase or spillover (active site exchange for NO_2) on In sites. The deactivating effect of water can be explained by the alteration of the hydroxyl group balance on the surface thus limiting the partial

oxidation of HCs and the formation nitrogen–carbon and nitrogen–hydrogen containing species. In₂O₃ will easily form InO⁺ in dry conditions but the presence of water favors less active In₂O₃.

3.5. Kinetic model for In/ZSM-5

The effects of residence time in the catalyst bed and the composition of feed flow were studied on In/ZSM-5 in dry conditions. The parameters are based on the set of these experiments, where NO, CH₄ and O₂ concentrations as well as SV and temperature were varied in practical steady state conditions. According to the standard experiment at the beginning and at the end of experimental sequence, the activity level was the same all times. Thus, the results depend only on kinetic factors but not on deactivation.

The highest NO reduction degree (over 90% NO_x conversion at 450–500 °C) in the kinetic experiments was attained with 500 ppm NO and 2500 ppm methane and the activity was higher particularly at lower temperatures (300–450 °C) compared to the conversions with lower CH₄/NO ratios. The same effect was seen also by later simulations, where these detected properties were included in kinetic parameters (Fig. 8). When relatively low CH₄ concentrations (500 ppm) were used, the methane oxidation rate was faster and thus the NO reduction efficiency was low compared to higher methane concentrations (1000 ppm). Oxygen has promoting effects on the reactions [6] but small differences were detected in the range of 4 and 10% O₂. The oxygen concentration was not so important at low temperatures but a lower oxygen concentration probably limited NO oxidation to NO₂ (no NO₂ in outlet) with the highest NO conversions.

The proposed mechanism includes reaction steps (1)–(5) and (10)–(17). The reaction steps (1)–(4) and (12) were assumed to be in quasi-equilibrium, and the steps (5) and (17) were assumed to be rate controlled, reversible reactions. The rest of the reaction steps were assumed to be irreversible. The steady-state kinetic model was derived as follows:

$$r_5 = \frac{k_5 K_{\text{NO}} K_{\text{O}_2}^{1/2} p_{\text{NO}} p_{\text{O}_2}^{1/2} \left(1 - \frac{K_{\text{NO}_2}^{\text{eq}} p_{\text{NO}_2}}{K_5^{\text{eq}} K_{\text{NO}} K_{\text{O}_2}^{\text{eq}} p_{\text{NO}} p_{\text{O}_2}^{1/2}} \right)}{D^2} \quad (18)$$

$$r_{10} = \frac{k_{10} K_{\text{CH}_4}^{\text{eq}} K_{\text{O}_2} p_{\text{CH}_4} p_{\text{O}_2}}{D^2} \quad (19)$$

$$r_{11} = \frac{k_{11} K_{\text{CH}_4}^{\text{eq}} K_{\text{NO}_2}^{\text{eq}} K_{\text{O}_2}^{1/2} p_{\text{CH}_4} p_{\text{O}_2}^{1/2} p_{\text{NO}_2}}{D^2} \quad (20)$$

$$r_{13} = \frac{((k_{13} K_{12} k_{10}) / (k_{15})) (K_{\text{NO}}^2 K_{\text{O}_2}^{1/2} K_{\text{CH}_4}^{\text{eq}}) / (K_{\text{NO}_2}^{\text{eq}}) (p_{\text{NO}}^2 p_{\text{O}_2}^{1/2} p_{\text{CH}_4}) / (p_{\text{NO}_2})}{D^2} + \frac{((k_{13} K_{12} k_{11}) / (k_{15})) K_{\text{NO}}^2 K_{\text{CH}_4}^{\text{eq}} p_{\text{NO}}^2 p_{\text{CH}_4}}{D^2} \quad (21)$$

$$r_{14} = \frac{k_{14}}{k_{13}} r_{13} \quad (22)$$

$$r_{15} = r_{10} + r_{11} \quad (23)$$

$$r_{16} = r_{15} + r_{17} \quad (24)$$

$$r_{17} = \frac{((k_{17}^- k_{10}) / (k_{16})) K_{\text{O}_2}^{1/2} K_{\text{CH}_4}^{\text{eq}} p_{\text{O}_2}^{1/2} p_{\text{CH}_4}}{D} + \frac{((k_{17}^- k_{11}) / (k_{16})) K_{\text{CH}_4}^{\text{eq}} K_{\text{NO}_2}^{\text{eq}} p_{\text{CH}_4} p_{\text{NO}_2}}{D} \quad (25)$$

$$D = 1 + K_{\text{NO}} p_{\text{NO}} + K_{\text{O}_2}^{1/2} p_{\text{O}_2}^{1/2} + K_{\text{NO}_2}^{\text{eq}} p_{\text{NO}_2} + \left(K_{\text{CH}_4}^{\text{eq}} K_{\text{O}_2}^{1/2} + \left(1 + \frac{k_{15}}{k_{16}} \right) \frac{k_{10} K_{\text{CH}_4}^{\text{eq}} K_{\text{O}_2}^{1/2}}{k_{15}} \right) p_{\text{CH}_4} p_{\text{O}_2}^{1/2} + \left(1 + \frac{k_{15}}{k_{16}} \right) \frac{k_{11}}{k_{15}} K_{\text{CH}_4}^{\text{eq}} K_{\text{NO}_2}^{\text{eq}} p_{\text{CH}_4} p_{\text{NO}_2} + \frac{K_{12} k_{10}}{k_{15}} \frac{K_{\text{NO}} K_{\text{O}_2}^{1/2} K_{\text{CH}_4}^{\text{eq}} p_{\text{NO}} p_{\text{O}_2}^{1/2} p_{\text{CH}_4}}{K_{\text{NO}_2}^{\text{eq}} p_{\text{NO}_2}} + \frac{K_{12} k_{11}}{k_{15}} K_{\text{NO}} K_{\text{CH}_4}^{\text{eq}} p_{\text{NO}} p_{\text{CH}_4} \quad (26)$$

After re-parameterization and sensitivity analysis, the kinetic equations used in the final parameter estimation became as follows:

$$r_5 = \frac{k_{51} p_{\text{NO}} p_{\text{O}_2}^{1/2} \left(1 - \frac{1}{K_{51}^{\text{eq}}} \frac{p_{\text{NO}_2}}{p_{\text{NO}} p_{\text{O}_2}^{1/2}} \right)}{D^2} \quad (27)$$

$$r_{10} = \frac{k_{101} p_{\text{CH}_4} p_{\text{O}_2}}{D^2} \quad (28)$$

$$r_{11} = \frac{k_{111} p_{\text{CH}_4} p_{\text{O}_2}^{1/2} p_{\text{NO}_2}}{D^2} \quad (29)$$

$$r_{13} = \frac{k_{131} p_{\text{NO}}^2 p_{\text{CH}_4}}{D^2} \quad (30)$$

$$r_{14} = k_{141} r_{13} \quad (31)$$

$$r_{17} = 0 \quad (32)$$

$$D = 1 + K_{\text{sqH}_2\text{O}} p_{\text{O}_2}^{1/2} + K_{\text{NO}_2}^{\text{eq}} p_{\text{NO}_2} \quad (33)$$

Thus, the formation rates of gas phase components are $(\partial p_{\text{N}_2} / \partial t) = r_{13}$, $(\partial p_{\text{NO}_2} / \partial t) = r_5 - r_{11}$, $(\partial p_{\text{N}_2\text{O}} / \partial t) = r_{14}$, $(\partial p_{\text{NO}} / \partial t) = -r_5 - 2r_{13} - 2r_{14} + r_{11}$, $(\partial p_{\text{O}_2} / \partial t) = -(1/2)r_5 - 2r_{10} - (3/2)r_{11} + r_{13} + (1/2)r_{14}$, $(\partial p_{\text{CH}_4} / \partial t) = -r_{10} - r_{11}$, $(\partial p_{\text{CO}_2} / \partial t) = r_{10} + r_{11}$ and $(\partial p_{\text{H}_2\text{O}} / \partial t) = 2r_{10} + 2r_{11}$.

The catalyst bed was supposed to operate as a steady-state plug flow reactor. The system of ordinary differential equations was solved by a stiff ODE solver (LSODE) using the backward difference method. The Nelder–Mead simplex and Levenberg–

Marquardt algorithms were used in the parameter estimation. Reaction rate parameters and equilibrium constants are temperature-dependent with constant activation energies and reaction enthalpies. However, parameters k_{141} and $K_{\text{NO}_2}^{\text{eq}}$ were

supposed to be temperature-independent. The values of parameters (K_{51}^{eq} and $\Delta\tilde{H}_{51}$), which describe the equilibrium between NO and NO₂, were fitted on the data calculated in a HYSYS process simulation program with fully thermodynamic information. The rest of parameters were estimated simultaneously based on kinetic experiments. The estimated relative standard errors of parameters were between 4 and 30%. The model explained the data as a R^2 value of 96%.

The prepared model was also verified by comparing the simulated and measured concentration responses in the experiments used for parameter estimation. The deviation between measured and simulated concentrations was negative or positive depending on the conditions. The simulated values were calculated by the interval of 12.5 °C between 200 and 600 °C (experiments at 250–550 °C by 50 °C intervals) showing the possibility of interpolation and extrapolation by simulations (Fig. 7). In fact, the extrapolation showed finely the assumed directions of the responses, e.g. a decrease of the N₂ concentration between 550 and 600 °C when the CH₄ oxidation was becoming too fast. The interesting N₂ concentration was predicted well but the simulation predicted a slightly lower CH₄ oxidation at 350–450 °C compared to the detected values. In the shown example, F/W was higher (60 dm³ h⁻¹ g⁻¹, direct relation to SV) than in the standard reaction mixture, which kept the conversions in moderate level (maximum N₂ formation of 60% at 500 °C). When F/W was as high as 240 dm³ h⁻¹ g⁻¹, maximum N₂ formation was decreased to 32%.

The thoroughness of the developed model was also evaluated by simulating responses in unmeasured conditions (1000 ppm NO, 1000 or 1500 ppm CH₄, 10% O₂, 60 dm³ h⁻¹ g⁻¹), which simulation predicted a higher N₂ formation (maximum about 70%) with 1500 ppm CH₄ (Fig. 8). Therefore the model forecasted the potential of NO_x reduction by higher CH₄/NO_x ratios. The effect of NO₂ on the enhanced CH₄ oxidation rate was also seen by a simulation in the same condition but the enhanced N₂ formation by 30% of NO₂ in the feed was not clearly predicted by this model. NO₂ was present only as an experiment. Thus kinetic parameters were mainly

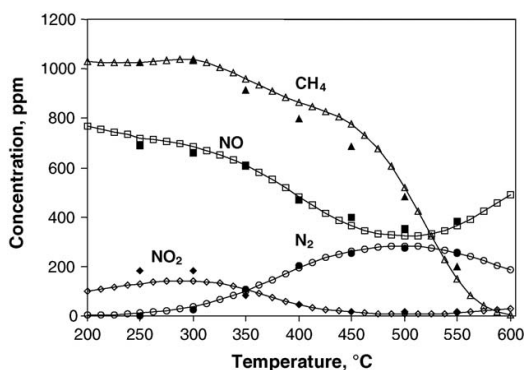


Fig. 7. Measured (solid points) and simulated (lines) gas phase compounds in In/ZSM-5 catalyst reactor outlet on as a function of temperature (1000 ppm NO, 1000 ppm CH₄, 10% O₂, $F/W = 60$ dm³ h⁻¹ g⁻¹).

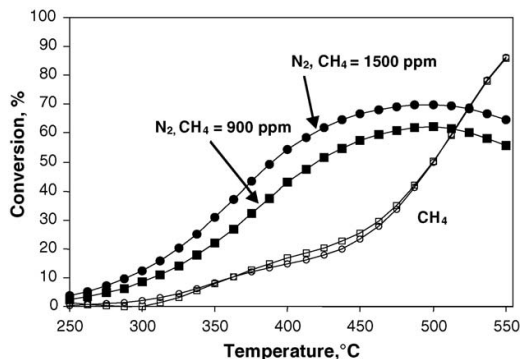


Fig. 8. The simulated N₂ formation and CH₄ conversion with two different CH₄ inlet concentrations (1000 ppm NO, 900 (square) or 1500 ppm (circle) CH₄, 10% O₂, $F/W = 60$ dm³ h⁻¹ g⁻¹).

estimated with NO–CH₄–O₂ mixtures, where the simulations gave relatively good predictions. The modification of our model to make a clearer kinetic difference between NO and NO₂ in reaction mechanism will be done in another study, where the effect of NO₂ will be examined more in details. The rate equations showed the dependency of reaction rates on partial pressures (concentrations) of NO, CH₄, O₂ and NO₂ in the gas phase. A difference to power law models, found in published literature for this reaction, is the fact that our equations were derived completely by the observed and assumed reaction mechanisms including surface steps. When the complete rate equations including surface reactions were first made, certain simplifications can be assumed. The presented model did not contain many simplifications in respect of the chosen reaction mechanism but our simplifications are the assumptions that the other parallel reaction paths can be excluded in the kinetic model and reactions will proceed in certain orders. We found that the derived model simulated well these reaction dynamics with the simplifications applied. The proposed actual reductant (NCH₂O*) is a representative for any kind of N containing species where N–O bonding is already cut and which could reduce NO in surface reaction. Other parallel similar reductants can be adsorbed HNCO, NCO, NH₂, NH or N, which are formed from H₂NCO by the releases of water and CO₂ in partial oxidation reactions. The possible N₂O₄ type paths [48] for NO_x reduction was neglected in our model and we thus assumed that the formation of a N–N bonding is completely taking place after the breakage of two N–O bonds. Gaseous NO₂ has known to also have a great oxidation ability [49] but our reaction mechanism assumed adsorbed NO₂ to be the oxidizing reactant (Langmuir–Hinshelwood mechanism).

The model enabled us to make simulations as a function of the catalyst reactor length (Fig. 9). The effect of temperature on the N₂ formation from NO_x was simulated at 350, 450 and 550 °C. The CH₄ oxidation and N₂ formation reactions are very slow at 350 °C and the N₂ formation could be increased by using larger reactor volumes. Oppositely, CH₄ is consumed fast at 550 °C and the maximum N₂ was already reached after the dimensionless length of 0.6 ($\rightarrow F/W$ about 30 dm³ h⁻¹ g⁻¹ needed to maximum N₂ and full methane conversions).

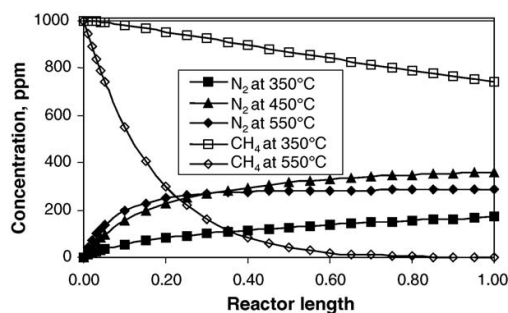


Fig. 9. The simulated concentrations of N_2 and CH_4 as a function of a length on In/ZSM-5 catalyst reactor at 350, 450 and 550 °C (Inlet: 1000 ppm NO, 1000 ppm CH_4 , 10% O_2 , up to $F/W = 20 \text{ dm}^3 \text{ h}^{-1} \text{ g}^{-1}$ corresponding to the dimensionless length of 1.00).

The design of catalyst reactors could be based on this kind of simulation. The required low temperature activity dictates the minimum catalyst amount. The model predicts that the active sites are occupied by adsorbed oxygen (O^*) and NO_2^* , in addition of free vacants (Fig. 10). The coverage of other surface intermediates was very low. Thus their lifetime was short and they were consumed in reaction sequences. The amount of free vacant was highest in inlet and at lower temperatures. NO_2^* and free vacant are replaced by O^* , when temperature increased. A chemical explanation for this simulation result can be understood if we assume the higher temperature to enhance the oxidation of active sites. The simulated balance between $O^* \leftrightarrow NO_2^*$ on sites matches well to the thermodynamic facts. It was not possible to detect O^* by FTIR studies. Even if the In state was detected by XPS and XRD on fresh samples at room temperature, the relevant oxidation state was not detected in situ during reactions. Thus these dynamic simulations gave a good addition to surface characterizations to interpret the reaction mechanism or even surface complexes. Chemically adsorbed O^* can be understood as an oxidation state of In oxides.

Probably we should stay relatively near to the experimental values in extrapolations with this kind of model related to the

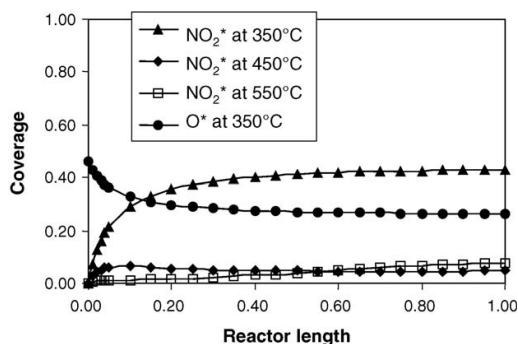


Fig. 10. Surface coverages of NO_2^* and O^* axially in In/ZSM-5 catalyst reactor at 350, 450 and 550 °C (Inlet: 1000 ppm NO, 1000 ppm CH_4 , 10% O_2 , up to $F/W = 20 \text{ dm}^3 \text{ h}^{-1} \text{ g}^{-1}$ corresponding to the dimensionless length of 1.00).

complicated reaction mechanisms. However, the conditions in practical lean CH_4 applications cannot be very different. If the conditions are stoichiometric or rich, the reaction mechanisms will change completely and these models cannot be used.

4. Conclusions

Indium on protonated H-ZSM-5 showed higher activity in dry conditions for NO reduction by CH_4 in lean conditions in the presence of O_2 than indium on unprotonated ZSM-5. However, the latter which had a higher indium loading, had a higher activity under wet conditions. The presence of NO_2 in the feed significantly enhanced the reaction rate to N_2 . It was proposed and detected by XRD and XPS that intrazeolitic InO^+ is the active site for NO reduction and separate In_2O_3 particles might promote NO_2 formation particularly in wet conditions. The number of InO^+ sites is assumed to decrease in wet conditions, where the activity for NO_x reduction was clearly decreased. Static and dynamic in situ FTIR experiments mostly revealed the existence of inhibiting compounds like nitrates and carbonates at lower temperatures. Carbonaceous compounds in the majority and N containing surface compounds in the minority appeared under reaction conditions at 350–480 °C. The observations proved the difficulty of the CH_4 activation to form surface species and low surface coverage of any surface compound under the reduction conditions giving the highest NO conversion.

A micro kinetic model based on surface reaction mechanism was developed for the In/ZSM-5 catalyst in this reaction. The adsorbed H_2NCO intermediate, formed by the reaction between NO_2 and partially oxidized methane, was proposed to be the actual NO reductant in the mechanism, which was good enough to explain and simulate quantitatively these catalytic reactions. The responses of NO, CH_4 , NO_2 , N_2 , N_2O , CO_2 and H_2O in the gas phase as well as defined surface coverage were predicted by the simulations in reactor outlet or as a function of temperature and reactor length. It was possible to predict reactants and product outlet concentrations after a catalyst reactor as NO reduction by CH_4 in the presence of excess oxygen under steady state conditions differently from those used in parameter estimation experiments. These surface reaction simulations also predicted the existence of adsorbed NO_2^* below 350 °C and a higher coverage of adsorbed O^* at higher temperatures matching the observations.

Acknowledgments

The experiments were carried out in a visiting researcher program funded by AIST. In addition, the authors are grateful to Cosmo Oil R&D Center for accomplishing the XPS and plasma analysis.

References

- [1] Y. Sato, H. Yu-u, N. Mizuno, M. Iwamoto, Appl. Catal. 70 (1991) L1.
- [2] H. Hamada, Y. Kintaichi, M. Sasaki, T. Itoh, M. Tabata, Appl. Catal. 64 (1990) L1.

- [3] M. Iwamoto, H. Hamada, *Catal. Today* 10 (1991) 57.
- [4] Y. Nishizaka, M. Misono, *Chem. Lett.* (1993) 1295.
- [5] B.J. Adelman, W.M.H. Sachtler, *Appl. Catal. B* 14 (1997) 1.
- [6] L.J. Lobree, A.W. Aylor, J.A. Reimer, A.T. Bell, Oral presentation at 2nd World Congress on Environmental Catalysis, Miami, 1998 (Abstract 1-3).
- [7] Y. Li, J.N. Armor, *J. Catal.* 145 (1994) 1.
- [8] Y. Li, J.N. Armor, *Appl. Catal. B* 1 (1992) L31.
- [9] Y. Li, J.N. Armor, *Appl. Catal. B* 3 (1993) L1.
- [10] K. Yogo, S. Tanaka, M. Ihara, T. Hishiki, E. Kikuchi, *Chem. Lett.* (1992) 1025.
- [11] K. Yogo, M. Ihara, I. Terasaki, E. Kikuchi, *Appl. Catal. B Environ.* 2 (1993) L1.
- [12] E. Kikuchi, K. Yogo, *Catal. Today* 22 (1994) 73.
- [13] E. Kikuchi, M. Ogura, *Catal. Surv. Jpn.* 1 (1997) 227.
- [14] M. Ogura, M. Hayashi, E. Kikuchi, *Catal. Today* 45 (1998) 139.
- [15] M. Ogura, Y. Sugiura, M. Hayashi, E. Kikuchi, *Catal. Lett.* 42 (1996) 185.
- [16] A.R. Beltramore, L.B. Pierella, F.G. Requejo, O.A. Anunziata, *Catal. Lett.* 91 (1–2) (2003) 19.
- [17] L. Ren, T. Zhang, C. Xu, L. Lin, *Top. Catal.* 30–31 (2004) 55–57.
- [18] T. Sowade, C. Schmidt, F.W. Schutze, H. Berndt, W. Grunert, *J. Catal.* 214 (1) (2003) 100–112.
- [19] J.A.Z. Pieterse, E.W. van den Brink, S. Booneveld, F.A. Bruijn, *Appl. Catal. B* 46 (2003) 239–250.
- [20] T. Sowade, F.W. Schutze, H. Berndt, W. Grunert, *Chem. Eng. Technol.* 27 (12) (2004) 1277–1289.
- [21] R. Burch, S. Scire, *Appl. Catal. B* 3 (1994) 295.
- [22] A.W. Aylor, L.J. Lobree, J.A. Reimer, A.T. Bell, *J. Catal.* 170 (1997) 390.
- [23] Z. Li, M. Flytzani-Stepanopoulos, *Appl. Catal. A* 165 (1997) 15.
- [24] M.W. Kumthekar, U.S. Ozkan, *J. Catal.* 171 (1997) 45.
- [25] C. Shi, A.B. Walters, M.A. Vannice, *Appl. Catal. B* 14 (1997) 175.
- [26] X. Zhang, A.B. Walters, M.A. Vannice, *Appl. Catal. B* 7 (1996) 321.
- [27] X. Zhang, A.B. Walters, M.A. Vannice, *J. Catal.* 155 (1995) 290.
- [28] M. Misono, *Cattech* 2 (1) (1998) 53.
- [29] M. Inaba, Y. Kintaichi, H. Hamada, *Catal. Lett.* 36 (1996) 223.
- [30] H. Hamada, *Catal. Surv. Jpn.* 1 (1996) 53.
- [31] T. Maunula, Y. Kintaichi, M. Inaba, M. Haneeda, K. Sato, H. Hamada, *Appl. Catal. B* 15 (1998) 291.
- [32] M. Shelef, *Chem. Rev.* 95 (1995) 209.
- [33] T. Yamashita, A. Vannice, *J. Catal.* 163 (1996) 158.
- [34] T. Maunula, Y. Kintaichi, M. Haneda, H. Hamada, *Catal. Lett.* 61 (1999) 121.
- [35] C. Schmidt, T. Sowade, E. Löffler, A. Birkner, W. Grunert, *J. Phys. Chem. B* 106 (2002) 4085–4097.
- [36] I.V. Yentejakis, R.M. Lambert, M. Konsolakis, V. Kiouisis, *Appl. Catal. B* 18 (1998) 293.
- [37] M. Misono, S. Yokoyama, G. Koyano, Oral presentation at 2nd World Congress on Environmental Catalysis, Miami, 1998 (Abstract 9-3).
- [38] E. Kikuchi, M. Ogura, I. Terasaki, Y. Goto, *J. Catal.* 161 (1996) 465.
- [39] M. Ogura, M. Hayashi, E. Kikuchi, *Catal. Today* 42 (1998) 159.
- [40] H. Chen, El-Malki, X. Wang, R. van Santen, W. Sachtler, *J. Mol. Catal. A* 162 (2000) 159.
- [41] R. Burch, D.J. Crittle, M.J. Hayes, *Catal. Today* 47 (1999) 229.
- [42] J. Halasz, Z. Konya, A. Fudala, A. Beres, I. Kiricsi, *Catal. Today* 31 (1996) 293.
- [43] L.G. Pinaeva, E.M. Sadovskaya, A.P. Suknev, V.B. Goncharov, V.A. Sadykov, B.S. Balzhinimaev, T. Decamp, C. Mirodatos, *Chem. Eng. Sci.* 54 (1999) 4327.
- [44] K. Tabata, Y. Yeng, T. Takemoto, E. Suzuki, M.A. Banares, M.A. Pena, J.L.G. Fierro, *Catal. Rev.* 44 (2002) 1–58.
- [45] T. Maunula, J. Ahola, H. Hamada, *Appl. Catal. B* 26 (2000) 173.
- [46] V. Zuzaniuk, F.C. Meunier, J.R.H. Ross, *J. Catal.* 202 (2001) 340–353.
- [47] E.A. Lombardo, G.A. Sill, J.L. d'Itri, W.K. Hall, *J. Catal.* 173 (1998) 440–449.
- [48] T. Maunula, J. Ahola, T. Salmi, H. Haario, M. Härkönen, M. Luoma, V.J. Pohjola, *Appl. Catal. B* 12 (1997) 287.
- [49] Z. Yan, C.-X. Xiao, Y. Kou, *Catal. Lett.* 85 (2003) 135.